Fire Technology
© 2015 Springer Science+Business Media New York (Outside USA).
Manufactured in The United States
DOI: 10.1007/s10694-015-0543-5

Burning Rates of Wood Cribs with Implications for Wildland Fires

Sara McAllister and Mark Finney, USDA Forest Service, RMRS Missoula Fire Sciences Lab, 5775 W US Highway 10, Missoula, MT 59808, USA*

Received: 7 August 2015/**Accepted:** 31 October 2015

Abstract. Wood cribs are often used as ignition sources for room fire tests and the well characterized burning rates may also have applications to wildland fires. The burning rate of wildland fuel structures, whether the needle layer on the ground or trees and shrubs themselves, is not addressed in any operational fire model and no simple model exists. Several relations exist in the literature for the burning rate of wood cribs, but the cribs used to generate them were built with fairly limited geometries. This work explores the burning rate of cribs with a wide variety of geometries and aspect ratios in the loosely-packed regime to evaluate the rigor of several correlations from the literature. Specifically, stick thicknesses ranged from 0.16 cm to 1.27 cm and lengths from 6.4 cm to 61.0 cm resulting in aspect ratios (stick length/thickness) from 10 cm to 160. As wildland fuel beds occur both directly on the ground and suspended in the air, the effect of the vertical gap between the ground and crib base was also examined. The critical vertical gap was shown to be larger than previously thought (7.6 cm for all cribs) and a function of the aspect ratio. It was quite apparent that as the aspect ratio increases, a significant portion of the required oxidizer comes from the bottom of the crib. A relation is then found to adjust the predicted values for the reduction in burning rate due to insufficient vertical gap.

Keywords: Burning rate, Cribs, Porosity, Vertical gap, Wildland fire

List of Symbols

a_v	Area of single vertical shaft (s^2) (cm^2)
a_s	Surface area of single vertical shaft (4 sh) (cm^2)
A_v	Total area of vertical shafts (cm^2)
A_s	Total stick surface area (cm^2)
b	Stick thickness (cm)
B	Enthalpy ratio (Eq. 13) (dimensionless)
c_p	Specific heat (kJ/kg K)
C	Fuel property constant in Block's Theory (Eq. 3) ($g/s*cm^{1.5}$)
d	Height above ground of crib bottom (cm)
f	Friction factor (dimensionless)
F	Ratio of the thermal diffusivity of Douglas-fir to the wood tested (dimensionless)
g	Acceleration due to gravity (m/s^2)
G	Modified Froude number defined in Eq. 6 (dimensionless)
h	Crib height (cm)
H_c	Heat of combustion of pyrolyzates (kJ/kg)

* Correspondence should be addressed to: Sara McAllister, E-mail: smcallister@fs.fed.us

Published online: 12 December 2015

H_p	Heat required for pyrolysis (kJ/kg)
l	Crib/stick length (cm)
n	Number of sticks per layer (dimensionless)
N	Number of layers (dimensionless)
P	Perimeter of vertical shaft (4s) (cm)
R	Burning rate (g/s)
R_{max}	Maximum burning rate measured for a given crib design (g/s)
s	Spacing between sticks (cm)
T_s	Temperature in shaft (°C)
T_0	Ambient temperature (°C)
γ	Fuel-to-air mass ratio for pyrolyzate-air reaction (dimensionless)
λ	Ratio of gas mass flux leaving to air entering (Eq. 16) (dimensionless)
φ_{Gross}	Crib porosity as defined by Gross (Eq. 1) ($cm^{1.1}$)
$\varphi_{Heskestad}$	Crib porosity as defined by Heskestad (Eq. 7) (cm)
ν_∞	Kinematic viscosity of ambient air (m^2/s)
ρ	Density of air in the vertical shafts (kg/m^3)
ρ_0	Density of ambient air (kg/m^3)
Ψ	Drag coefficient defined in Eq. 5 (dimensionless)

1. Introduction

Wood cribs are often used as ignition sources in room fire tests (for example in UL 1715 and ISO 9705 test standards) and for various other tests requiring repeatable heat release rates, such as fire extinguisher performance (ANSI/UL 711). To vary the burning rate of the source fire, cribs can be built with different stick thicknesses and arrangements. Thus predicting the burning behavior of a crib a priori can be particularly useful when designing a new testing procedure (see for example [1–4]).

The prediction of the burning rate of a crib may also have applications outside of fire testing. The burning rate of wildland fuels, both in the litter layer on the forest floor and the trees and shrubs themselves, is not well understood. Operational fire models in Australia and Canada are purely empirical, predicting rate of spread based completely on field measurements [5, 6]. Operational fire models in the United States, such as BEHAVEPlus [7, 8] and FARSITE [9], while including some basic quasi-physical relations [10], only predict fire spread rates and do not directly calculate the burning rate of wildland fuel beds. Though challenging to define [11] and not actually used to calculate the rate of spread, these operational models predict the related quantity of "flame residence time." Logically residence time should be approximately equal to the mass of fuel burned in the flaming phase divided by the burning rate. The simple relationship used in the operational models in the United States is that the residence time is equal to eight times the diameter of the fuel in inches [12, 13]. Clearly, such a simple relationship does not include nearly all of the parameters known to affect the burning rate of porous fuel beds, such as porosity and any ventilation effects. FARSITE and FOFEM (First-Order Fire Effects Model, another model developed in the United States) have an additional burnout model for the large woody material that continues to burn after the main fire front [9, 14]. This model is based on the work of Albini

and others [15, 16]. While based on physical equations, this burnout model makes many unverified simplifying assumptions and relies very heavily on several empirical constants. In [11], Nelson modified the models of Albini [15, 17] to include effects of the ventilation and surface-area controlled regimes. By doing so, he was able to predict the residence time and burning rate on a surface-area basis with reasonable accuracy for pine needle beds. Unfortunately, the model did not perform well for beds of vertical wood dowels. Also problematic was the prediction of the transition between burning regimes and the burning rate on a horizontal surface-area basis.

Recently, an effort has been made to measure the burning and heat release rate of piles of needles and leaves. For example, Burrows studied the residence time and burning rate of both individual and piles of eucalyptus leaves and twigs [18] though no attempt was made to control or even describe parameters such as the density or porosity of the piles. In this study, the flame residence time of round wood dowels was seen to be proportional to the diameter raised to some power. For individual dowels, this power was 1.875, while for piles it was 1.236. For loosely-packed fuel beds, this power has also been reported to be 1.5 in [19, 20] and 2 in [21]. Even if wildland fuel beds are always well ventilated and burning in the surface-area controlled regime, it is not clear that the residence time is the simple linear relationship with the diameter from Anderson [12] that is used in many operational wildfire models.

The more sophisticated techniques available from the fire protection engineering community have also been recently applied to wildland fuels. The cone calorimeter has been used on many species of wildland fuels, but the main goal of these research efforts was to use the heat release rate as a means to rank the flammability of vegetation [22, 23]. Wildland fuels have also been studied using the Fire Propagation Apparatus (FPA) in [24–27]. These studies included a custom-made permeable basket that allowed for the variation of airflow through the bed. Different burning behavior was seen from different species of seemingly similar pine needles. Though these behaviors were primarily attributed to physical, and not chemical, differences [27] it is difficult to completely isolate these effects while working with the actual needles. While demonstrating that the fuel bed permeability and mean free path of the radiation are primary drivers of the burning and heat release rate [27], these studies have not resulted in an a priori method of prediction of any form, numerical or empirical.

Even though wildland fuels do not have the same predictable arrangement as wood cribs, it is possible that an understanding of the factors that govern the burning rate of a crib will apply to the wildland fire context [19, 28, 29]. After all, all wildland fuels are essentially individual fuel particles with some spacing distance between them. By using relatively simple fuel beds, progress into understanding the burning behavior of more complex wildland fuels may finally be achieved.

2. Background

The first major exploration of the burning rate of cribs was conducted by Gross [30]. His cribs were primarily built from Douglas-fir with a moisture content of about 9%. The sticks used all had a length (l) equal to ten times the thickness (b) ($l/b = 10$) and all cribs were built with ten layers, making them cubes. In this pioneering work, Gross demonstrated that the burning rate of unconfined cribs occurs in two regimes: open or loosely-packed and closed or densely-packed. In the loosely-packed regime, the burning rate is more closely approximated by the free burning rate of the individual sticks and is governed by heat and mass transfer processes near the surfaces. In this regime, the burning rate is more of a function of the stick dimensions, and is independent of the "porosity" of the crib. For cribs in the densely-packed regime, the burning rate is limited by availability of oxidizer within the fuel bed. In this regime, the burning rate increases with the inter-stick spacing or the "porosity" of the crib. Gross defined the porosity of his cribs as

$$\varphi_{Gross} = N^{0.5} b^{1.1} \frac{A_v}{A_s} \tag{1}$$

where φ_{Gross} is the porosity ($\text{cm}^{1.1}$), N is the number of layers, b is the stick thickness (cm), A_s is the exposed surface area of the sticks (cm^2), and A_v is the area of the vertical shafts in the crib (cm^2). The scaled burning rate of his cribs was thus a function of this porosity as

$$FRb^{1.6} = fn\left[N^{0.5} b^{1.1} \frac{A_v}{A_s}\right] \tag{2}$$

where F is the ratio of the thermal diffusivity of Douglas-fir to the wood tested and R is the burning rate (g/s).

About a decade later, Block developed the first (and still only) theoretical model of the crib burning rate [31, 32]. Based on the observations of Gross [30], Block divided the burning rates into two regimes. In the loosely-packed regime, he assumed that the burning rate was closely related to the burning rate of the individual sticks. Based on a Spaulding's B number analysis, Block defined the burning rate of loosely-packed cribs as

$$\frac{R}{A_s} = Cb^{-0.5} \tag{3}$$

where C has units of ($\text{g/s cm}^{1.5}$) and varies for different wood species and moisture contents. In the densely-packed regime, Block assumed that the burning rate was controlled by the vertical movement of air and gaseous fuel and thus examined a single vertical vent of a crib. This vertical vent was treated as a porous tube with rough walls and a constant friction factor for this turbulent flow was measured to be $f = 0.13$. By considering the conservation equations for mass,

momentum, and energy, Block developed the following expression for the burning rate of cribs in the densely-packed regime

$$\frac{R}{A_s} = \frac{1}{2} f \rho \left\{ \left[\frac{\rho_0 - \rho}{\rho} \right] gh \right\}^{0.5} \left(\frac{\lambda - 1}{\lambda} \right) \frac{G}{\Psi} \tag{4}$$

where ρ is the density of air in the vertical shafts (g/cm^3), ρ_0 is the density of ambient air (g/cm^3), g is the acceleration due to gravity (cm/s^2), h is the height of the crib (cm), λ is the ratio of the mass flux of gases leaving to the mass flux entering a volume (dimensionless), and G and Ψ are as defined below.

$$\Psi = \frac{Phf}{2A_v} = \frac{(4s)hf}{2s^2} = 2\frac{h}{s} f \tag{5}$$

$$G = \left\{ \Psi^{-1} \left[\frac{1 - e^{-\Psi}}{1 - \left(\rho / \rho_0 \right)^2 \lambda^{-2} e^{-\Psi}} \right] \right\}^{0.5} \tag{6}$$

where s is the spacing between sticks (cm).

Block compared his model to experimental results he obtained by burning cribs with ponderosa pine sticks of a wide range of moisture contents. These sticks had lengths ranging from 10 to 20 times the stick thickness (l/b = 10–20). Block provided values of the coefficient C that best fit the experimental data. In one series of experiments of five crib designs with an aspect ratio (l/b) of 10, Block examined the effect of varying the vertical gap between the crib and the support platform (d). A maximum change in the burning rate of 15% was noted as the gap increased from 0.159 cm (1/16'') to 1.27 cm (0.5''), with no further changes as the gap was increased further.

Because Block's model was ''awkward'' to use, Heskestad [33] combined the experimental results from Gross [30] and Block [31, 32] with the theoretical findings of Block to develop a new correlation of the data in the more user-friendly form of Gross' original correlation:

$$\frac{R}{A_s b^{-1/2}} = fn \left[\left(\frac{A_v}{A_s} \right) s^{1/2} b^{1/2} \right] \tag{7}$$

The right hand side of the equation defines the porosity of the crib according to Heskestad ($\varphi_{\text{Heskestad}}$). This relation predicted the burning rates of the cribs burned in both [30] and [31, 32] well (±20%).

All three models for the burning rate of cribs discussed so far have been based on experiments with fairly limited geometries and aspect ratios (l/b). Unfortunately, wildland fuel beds will, by necessity, be represented by cribs with a wide range of external dimensions and aspect ratios (l/b). Only a few others have considered a wider range of crib geometries. Delichatsios tested cribs with aspect

ratios (l/b) up to 40, but ignited the cribs in the center to measure the growth rate of the spread [34]. Byram et al. [28] tested the effect of crib footprint area by keeping the stick spacing (s) and crib height constant and increasing the length of the sticks. The largest aspect ratio tested here was about 61. Byram successfully correlated his seven data points using dimensionless heat and mass transfer groups ($R/lv_\infty\rho_\infty \sim gl^3/v_\infty^2$). O'Dogherty and Young [35] tested a wide range of crib designs with aspect ratios up to 96, but their data are poorly predicted by any of the above models [36, 37], possibly for unspecified vertical gap (d) between the floor and the crib (as discussed below). Smith and Thomas [36] performed a statistical analysis of the data from O'Dogherty and Young [35], Gross (excluding the data from cribs with b = 0.16 cm) [30], and Webster (unpublished data) and recommended the correlation

$$\frac{R}{(A_s A_v h)} = \frac{0.0017}{(A_s A_v)^{0.052}} \tag{8}$$

using cgs units. Though the range of cribs that Byram [28] tested was small, his results also appear to fit this correlation as well. Upon reworking the results of Block, Thomas [37] later recommended correlating the data in the form

$$\frac{R}{A_s\rho_0(gh)^{0.5}} = 0.02\left(\frac{a_v}{a_s}\right)^{0.6} = 0.02\left(\frac{s^2}{4sh}\right)^{0.6} = 0.00388\Psi^{-0.6} \tag{9}$$

where a_v and a_s are the cross sectional area and surface area of a single vertical shaft and Ψ is from Eq. 5. While this correlation was more successful in correlating the data of O'Dogherty and Young [35] and Webster, Thomas excluded cribs with "a large ratio of horizontal to vertical dimensions" [37].

Another important aspect to consider for wildland fuels is the effect of the height of the fuel bed above the ground (vertical gap, d). Ground fuels, like the needle litter layer, have no way of supplying oxidizer through the bottom surface. On the other hand, crown fuels, like trees and shrubs, have ample oxidizer supply from the bottom. The effect of the vertical gap between the ground and crib base is not well explored as only one study exists for a small range of crib designs [31, 32].

This work explores the burning rate of cribs with a wide variety of geometries and aspect ratios to determine the most appropriate prediction tool for the burning rate of cribs likely to resemble wildland fuel beds. Wildland fuels are characterized by thin fuel elements (ex. pine needle diameter $b \sim 1$ mm) which results in fuel beds with a large aspect ratio (l/b). The effect of the vertical gap (d) is also considered for a wide range of crib designs.

3. Experiment Description

The experimental chamber used was very large (12.4 m × 12.4 m × 19.6 m) so that the airflow to the cribs was not restricted (unconfined). Three load cells spaced equally apart were used to continuously weigh the cribs during each test.

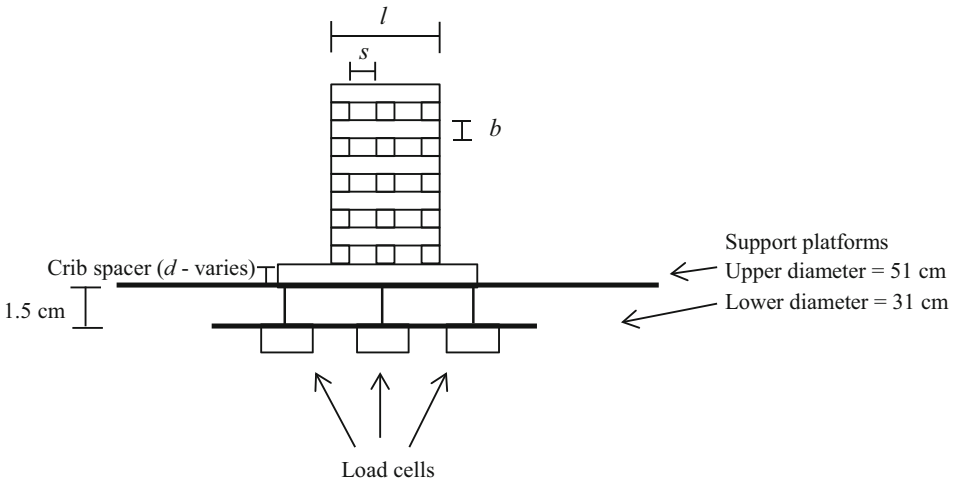

Figure 1. Sketch of apparatus for a crib with 3 sticks per layer (n = 3) and 10 layers (N = 10).

As shown in Figure 1, two thin aluminum discs, separated by pins to reduce heat transfer to the load cells, were used as a support platform for the cribs. Multiple sheets of ceramic paper insulation were placed on top of the support platform to further minimize heat transfer to the load cells. A thermocouple was located near the load cells to assure that the temperature remained fairly constant. All cribs were conditioned in an environmental chamber at 35°C and 3% relative humidity for at least 3 days, resulting in a calculated equilibrium moisture content of approximately 2.5%.

Simultaneous ignition of the cribs was achieved by quickly submerging the crib in 99% pure isopropyl alcohol and allowing it to drain. The total mass of fuel used was 10% or less of the crib weight. The liquid fuel was observed to easily burn off before the steady state burning of the crib was achieved. Both mass and temperature were logged at 2 Hz for the early tests, but the majority of the tests recorded data at 10 Hz. A sample of the raw data is shown in Figure 2, where four distinct phases of burning can be seen—burning off of the liquid fuel, stick ignition, steady burning, and burnout. Only data from the steady burning portion of the curve was used to calculate the burning rate. The burning rate was found from the slope of the best-fit line through the data.

Wood cribs were built using square ponderosa pine sticks with thicknesses ranging from 0.159 cm (1/16 in) to 1.27 cm (0.5 in). The first phase of experiments was performed to validate the testing apparatus against the known data of Gross [30]. Once the process was established, a wide variety of crib designs and vertical gaps between the ground and crib base (d) were explored. The loosely-packed regime was chosen because it was indicated by Fons et al. [19] that all wildland fuels would burn in this regime. The porosity factor of Heskestad [33] (Eq. 7) was kept approximately constant while the number of sticks per layer, number of layers and the length to thickness ratios (l/b) were varied. Table 1 shows the details of

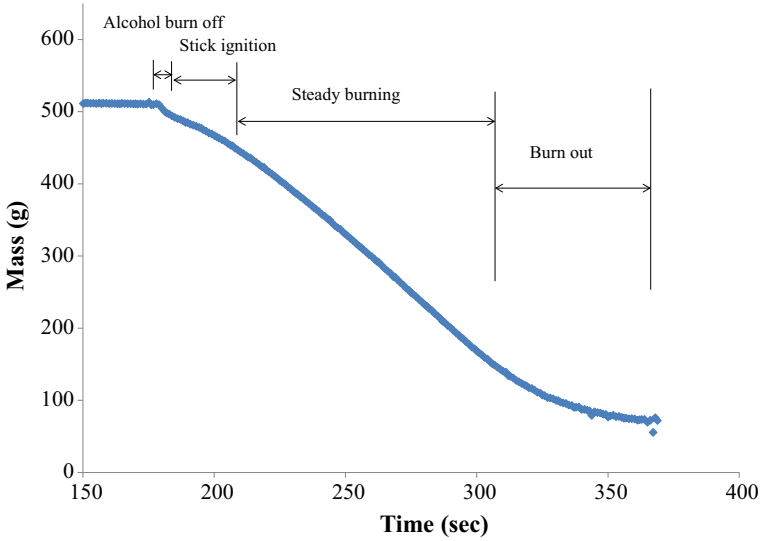

Figure 2. Sample raw data for crib design #8.

all cribs burned. As indicated in Table 1, the stick surface area and (l/b) were varied over an order or magnitude. The vertical gaps used between the ground and crib base (d) are also shown in Table 1. Crib designs in blue boxes were tested with vertical gaps of 0, 0.64, 1.27, 2.54, and 7.62. Otherwise, all cribs were tested with either 1.27 cm or 7.62 cm gaps as indicated. Each crib layout and vertical gap combination was tested three times and the results averaged.

4. Results and Discussion

The average burning rates of all cribs tested is listed in Table 2. Also listed in Table 2 are the standard deviation values as a percentage of the mean for each crib design and vertical gap tested. The average standard deviation for all tests was 5.6%, while the values ranged from 0.16% to 28.48%. The fit of the models of Heskestad [33], Block [31, 32], and Thomas [37] to the maximum burning rates for a given crib design will be compared in turn, followed by a discussion of the effect of the vertical gap between the ground and crib base (d). For the discussion of the models, the maximum burning rate was taken as the largest burning rate regardless of the vertical gap. For cribs with large l/b ratios (aspect ratios), this burning rate occurs at the largest vertical gap (d = 7.62 cm). For more standard, nearly cubic cribs, this occurs at a vertical gap of more like 1.27 cm to 2.54 cm.

4.1. Heskestad model

Figure 3 shows the maximum burning rate for each crib design against the Heskestad model [33]. In order to plot the Heskestad correlation and compare it to

Table 1
Crib Dimensions

Crib design	Stick thickness (b) [cm]	Stick length (l) [cm]	l/b [ ]	Number of sticks per layer (n) [ ]	Number of layers (N) [ ]	Surface area (A_s) [cm^2]	Heskestad Porosity (φ) [cm]
1	0.64	6.35	10	3	10	442.74	0.0530
2	0.64	6.35	10	5	10	665.32	0.0108
3	0.64	6.35	10	7	10	829.84	0.00196
4	1.27	12.7	10	3	10	1770.96	0.1060
5	1.27	12.7	10	5	10	2661.29	0.0215
6	1.27	12.7	10	7	10	3319.35	0.00393
7	0.64	6.35	10	2	12	370.97	0.1249
8	1.27	15.24	12	3	14	3009.67	0.117
9	0.64	10.16	16	2	30	1503.22	0.1249
10	0.64	10.16	16	3	12	878.22	0.126
11	0.64	10.16	16	4	6	574.19	0.1284
12	0.64	10.16	16	5	4	471.77	0.1089
13	0.64	10.16	16	6	2	290.32	0.1247
14	0.64	15.24	24	3	27	3012.09	0.1215
15	0.64	15.24	24	4	14	2045.16	0.129
16	0.64	15.24	24	5	9	1616.93	0.1246
17	0.64	15.24	24	6	6	1277.42	0.123
18	0.64	22.86	36	8	8	3406.45	0.118
19	0.64	30.48	48	8	14	8090.31	0.121
20	0.64	30.48	48	12	6	5051.60	0.119
21	0.32	15.24	48	6	12	1328.22	0.123
22	0.32	20.32	64	8	12	2354.83	0.121
23	0.32	20.32	64	14	4	1337.90	0.117
24	0.32	25.4	80	8	18	4454.83	0.119
25	0.32	25.4	80	14	6	2529.03	0.124
26	0.64	60.96	96	20	9	25435.43	0.116
27	0.32	30.48	96	8	24	7174.18	0.122
28	0.32	30.48	96	14	9	4586.68	0.118
29	0.16	15.24	96	9	10	838.76	0.119
30	0.16	15.24	96	3	70	2011.54	0.117
31	0.16	20.32	128	13	8	1287.55	0.127
32	0.16	20.32	128	15	36	6598.02	0.022
33	0.16	25.4	160	16	8	1980.64	0.130

Grey boxes indicate tests conducted with only 1.27 cm vertical gap between crib and ground. White boxes indicate tests conducted with only 7.62 cm gap. Blue boxes indicate tests conducted with all vertical gaps (0, 0.64, 1.27, 2.54, and 7.62 cm)

the experimental data, an approximation for the graphical form of the correlation was made. This approximation is

$$\frac{10^3 R}{C A_s b^{-0.5}} = 1 - \exp\left[-50\left(\frac{A_v}{A_s} s^{0.5} b^{0.5}\right)\right] \tag{10}$$

Table 2
Measured Burning Rates

Crib design	Vertical gap (d) [cm]	Heskestad Porosity (φ) [cm]	Block Porosity (Eq. 18) [ ]	Thomas Ψ (Eq. 15) [ ]	Average burning rate [g/s]	St dev (% of ave)[ ]	$10^3R/(A_sb^{-0.5})$ [g/s*cm$^{1.5}$]	$100R/(A_s\rho_o(gh)^{0.5})$ [ ]
1	1.27	0.0530	0.9343	0.7427	0.5249	5.46	0.9447	1.2940
2	1.27	0.0108	0.3486	2.0799	0.3569	5.11	0.4275	0.5856
3	1.27	0.0030	0.1066	5.2000	0.1523	0.60	0.0932	0.2003
4	1.27	0.1060	1.8684	0.7429	1.7407	1.88	1.1077	0.7586
5	1.27	0.0215	0.6972	2.0800	1.9199	2.94	0.8130	0.5568
6	1.27	0.0039	0.2132	5.2000	0.7077	2.00	0.2403	0.1645
7	1.27	0.1249	1.5438	0.3900	0.4985	8.80	1.1541	1.3388
8	0	0.1170	1.6767	1.0400	3.1546	-	1.1812	0.6837
	0.64	0.1170	1.6767	1.0400	3.1582	-	1.1826	0.6845
	1.27	0.1170	1.6767	1.0400	3.1036	6.14	1.1621	0.6727
	2.54	0.1170	1.6767	1.0400	3.1110	2.72	1.1649	0.6743
	7.62	0.1170	1.6767	1.0400	2.9653	3.04	1.1294	0.6427
9	1.27	0.1249	1.9805	0.5571	2.1564	4.12	1.1431	0.9040
10	1.27	0.1260	1.3743	0.4800	1.1570	3.85	1.0499	1.3127
11	1.27	0.1284	1.0916	0.3900	0.7465	0.90	1.0360	1.8319
12	1.27	0.1089	0.9057	0.3782	0.6017	2.61	1.0163	2.2010
13	1.27	0.1247	0.7598	0.2600	0.3475	5.43	0.9539	2.9216
14	1.27	0.1215	1.6590	0.6685	4.2433	8.02	1.1226	0.9358
15	0	0.129	1.3706	0.5460	2.2923	5.86	0.8932	1.0339
	0.64	0.129	1.3706	0.5460	2.7081	0.16	1.0552	1.2215
	1.27	0.129	1.3706	0.5460	2.8698	3.06	1.1182	1.2944
	2.54	0.129	1.3706	0.5460	2.8966	1.16	1.1286	1.3065
	7.62	0.129	1.3706	0.5460	2.7690	4.79	1.0789	1.2490
16	0	0.1246	1.1718	0.4926	1.6886	-	0.8322	1.2015
	1.27	0.1246	1.1718	0.4926	2.1625	2.90	1.0658	1.5388
	2.54	0.1246	1.1718	0.4926	2.3909	3.18	1.1783	1.7013
	7.62	0.1246	1.1718	0.4926	2.1322	10.35	1.0508	1.5172
17	1.27	0.123	1.0310	0.4333	1.6643	6.29	1.0382	1.8358
18	0	0.118	1.0687	0.5200	2.5748	2.82	0.6023	0.9224
	0.64	0.118	1.0687	0.5200	3.2772	8.98	0.7666	1.1740
	1.27	0.118	1.0687	0.5200	4.2010	7.35	0.9827	1.5050
	2.54	0.118	1.0687	0.5200	4.9931	2.48	1.1680	1.7887
	7.62	0.118	1.0687	0.5200	5.1495	1.82	1.2046	1.84476
19	0	0.121	1.2362	0.6370	8.3676	4.03	0.8242	0.9541
	1.27	0.121	1.2362	0.6370	10.8000	2.84	1.0638	1.2314
	2.54	0.121	1.2362	0.6370	12.4847	1.95	1.2297	1.4235
	7.62	0.121	1.2362	0.6370	12.3487	3.04	1.2163	1.4080
20	0	0.119	0.9758	0.4767	1.8780	11.93	0.2962	0.5239
	0.64	0.119	0.9758	0.4767	5.0705	-	0.7999	1.4144

The overall difference between the data and Heskestad model is 14.0% with a coefficient C of 1.08. Considering only the thin, 0.16 cm sticks, the model consistently overpredicts the burning rate by 44.4%. It is well known that as the porosity continues to increase past the loosely-packed region, eventually the burning rate will begin to decrease because the radiative heat exchange between fuel elements becomes inefficient. Very thin fuel elements are highly efficient in convective heat transfer (for example cooling fins), so one initial hypothesis was that this

Table 2
continued

	1.27	0.119	0.9758	0.4767	5.6618	8.61	0.8931	1.5793
	2.54	0.119	0.9758	0.4767	7.6376	5.48	1.2048	2.1304
	7.62	0.119	0.9758	0.4767	7.3315	10.56	1.1565	2.0451
21	0	0.123	0.7916	0.3714	1.0354	6.26	0.4392	1.0984
	0.64	0.123	0.7916	0.3714	1.5545	-	0.6595	1.6492
	1.27	0.123	0.7916	0.3714	1.8437	10.03	0.7822	1.9560
	2.54	0.123	0.7916	0.3714	1.9799	1.41	0.8399	2.1004
	7.62	0.123	0.7916	0.3714	2.3513	0.22	0.9975	2.4945
22	0	0.121	0.7571	0.4044	1.5185	5.74	0.3634	0.9087
	1.27	0.121	0.7571	0.4044	3.2181	3.59	0.7700	1.9257
	2.54	0.121	0.7571	0.4044	3.7264	2.28	0.8917	2.2298
	7.62	0.121	0.7571	0.4044	3.9658	4.30	0.9490	2.3731
23	7.62	0.117	0.5198	0.2817	2.6262	1.64	1.1061	4.7909
24	0	0.119	0.8684	0.4550	3.3809	5.30	0.4276	0.8732
	1.27	0.119	0.8684	0.4550	5.8874	8.95	0.7447	1.5205
	2.54	0.119	0.8684	0.4550	7.4509	1.57	0.9424	1.9243
	7.62	0.119	0.8684	0.4550	7.7295	2.97	0.9777	1.9963
25	7.62	0.124	0.6129	0.3073	4.8177	1.87	1.0734	1.9963
26	7.62	0.116	1.0505	0.5850	35.5367	21.14	1.0820	1.5622
27	7.62	0.122	0.9524	0.4964	13.0253	2.46	1.0230	1.8090
28	0	0.118	0.6860	0.3710	0.9620	7.27	0.1182	0.3413
	1.27	0.118	0.6860	0.3710	5.4751	9.97	0.6726	1.9423
	2.54	0.118	0.6860	0.3710	7.3941	5.32	0.9084	2.6230
	7.62	0.118	0.6860	0.3710	8.6751	1.77	1.0657	3.0774
29	0	0.119	0.4388	0.2391	0.4555	3.79	0.2164	1.1855
	0.64	0.119	0.4388	0.2391	0.8644	5.14	0.4106	2.2496
	1.27	0.119	0.4388	0.2391	1.2236	2.58	0.5813	3.1847
	2.54	0.119	0.4388	0.2391	1.3297	11.45	0.6316	3.4606
	7.62	0.119	0.4388	0.2391	1.3425	3.34	0.6377	3.4940
30	7.62	0.117	0.9304	0.3914	3.0234	12.42	0.5989	1.2401
31	0	0.127	0.4125	0.2080	0.2830	9.55	0.0876	0.5364
	1.27	0.127	0.4125	0.2080	1.7602	7.08	0.5447	3.3366
	2.54	0.127	0.4125	0.2080	1.9982	14.88	0.6183	3.7877
	7.62	0.127	0.4125	0.2080	2.3464	7.46	0.7261	4.4478
32	7.62	0.022	0.3044	1.1597	3.2865	28.48	0.1985	0.5731
33	0	0.130	0.4068	0.2167	0.5040	4.57	0.1014	0.6211
	1.27	0.130	0.4068	0.2167	2.3002	5.54	0.4627	2.8344
	2.54	0.130	0.4068	0.2167	3.2240	7.04	0.6486	3.9728
	7.62	0.130	0.4068	0.2167	3.6089	8.34	0.7260	4.4470

Grey boxes indicate tests conducted with only 1.27 cm gap between crib and ground. White boxes indicate tests conducted with only 7.62 cm gap. Blue boxes indicate tests conducted with all gaps (0, 0.64, 1.27, 2.54, and 7.62 cm)

burning rate limit is reached at a lower Heskestad porosity in the thin-stick case. To be certain that this wasn't the case, a densely-packed crib with a crib built with 0.16 cm sticks was tested. The burning rate of this densely-packed crib also fell below the predicted value from the Heskestad correlation. It appears then that the Heskestad correlation is robust for a wide range of crib designs and geometries as long as the stick thickness is 0.32 cm or greater. Unfortunately, the thickness of many wildland fuels (particularly pine needles) falls below this threshold thickness.

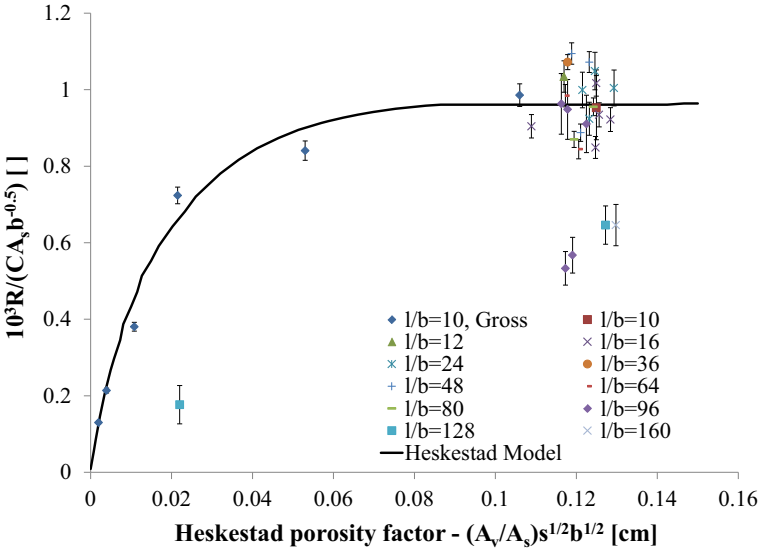

Figure 3. Measured maximum burning rate (R_{max}) compared to Heskestad model (Eq. 10).

4.2. Block Model

Figure 4 shows the maximum burning rate for each crib design against the Block model [31, 32]. In order to apply the Block model, the same constants and coefficients were used as in the original work. For convenience, they are presented here along with the simplified versions of Eqs. 4 to 6. Following [31, 32],

$$f = 0.13 \tag{11}$$

$$\sqrt{\rho(\rho_0 - \rho)} = 5.3 \times 10^{-4} \ \ [\mathrm{g/cm^3}] \tag{12}$$

$$B = \frac{H_c\gamma - c_p(T_s - T_0)}{H_p} = 2.6 \tag{13}$$

$$2/\left[1 + (\rho/\rho_0)\lambda^{-1}\right] = 1.84\,[\text{dimensionless}]$$
$$\Rightarrow \left(\frac{\rho}{\rho_0}\frac{1}{\lambda}\right)^2 = 7.561 \times 10^{-3}[\text{dimensionless}] \tag{14}$$

$$\Psi = \frac{Phf}{2A_v} = \frac{(4s)hf}{2s^2} = 2\frac{h}{s}f = 0.26\frac{h}{s} \tag{15}$$

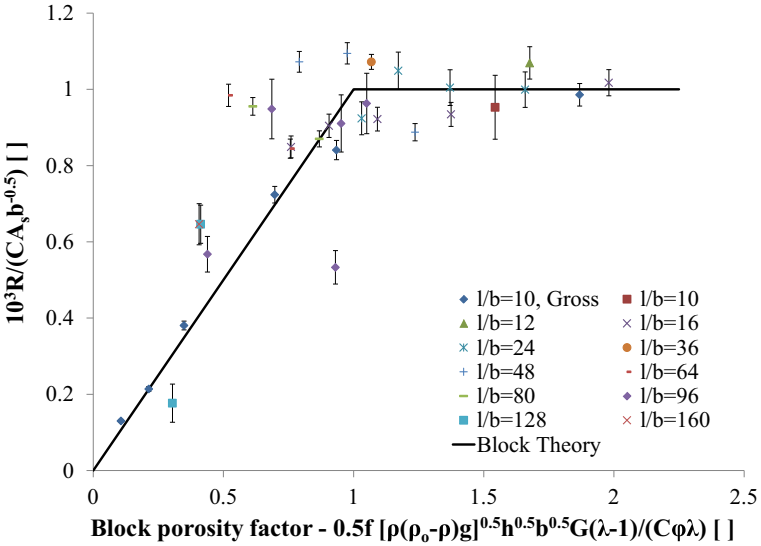

Figure 4. Measured maximum burning rate (R_{max}) compared to Block model (Eqs. 3, 11–18).

$$\frac{\lambda-1}{\lambda}=\frac{B}{(B+1)+\Psi^{-1}\left\{2/\left[1+(\rho/\rho_0)\lambda^{-1}\right]\right\}}=\frac{2.6}{3.6+1.84\Psi^{-1}} \tag{16}$$

$$G=\left\{\Psi^{-1}\left[\frac{1-e^{-\Psi}}{1-\left(\rho/\rho_0\right)^2\lambda^{-2}e^{-\Psi}}\right]\right\}^{0.5}=\left\{\Psi^{-1}\left[\frac{1-e^{-\Psi}}{1-7.561\times10^{-3}e^{-\Psi}}\right]\right\}^{0.5} \tag{17}$$

The x-axis in Block's plot of the model is then

$$\begin{aligned} x\text{-}axis &= \frac{f}{2}\frac{[\rho(\rho_0-\rho)g]^{0.5}}{C}h^{0.5}b^{0.5}\left(\frac{\lambda-1}{\lambda}\right)\frac{G}{\Psi} \\ &= 4.1479sh^{-0.5}b^{0.5}G\left(\frac{\lambda-1}{\lambda}\right) \end{aligned} \tag{18}$$

The overall difference between the data and the Block model is 17.3% with a coefficient C of 1.12. Block's model doesn't have such an obvious bias with the thin, 0.16 cm sticks—the model both under and overpredicts the burning rate. Interestingly, this lack of bias seems to be because of the difference in definition of the porosity. As mentioned above, all cribs were designed to have an approxi-

mately constant Heskestad porosity in the loosely-packed regime. As the sticks get very thin, the Block "porosity" (value of the x-axis, Eq. 18) decreases, so that cribs that are considered loosely-packed by Heskestad's definition are densely-packed by Block's. Unfortunately, while the model doesn't have an obvious bias, the error of the model increases to 45.9% for cribs built with these thin sticks. The Block model will, thus, also be unsuitable for wildland fuels.

4.3. Thomas Model

Figure 5 shows the data plotted as suggested by Thomas [37] (Eq. 9). The parameter Ψ is defined as above in Eq. 15. The best fit power law relation through the data is

$$\frac{100R}{A_s\rho_o(gh)^{0.5}} = 0.8499\Psi^{-0.97} \tag{19}$$

with an r^2 of 0.89. Though not the true best-fit curve, the simple relation shown below seems to predict the burning rate well.

$$\frac{100R}{A_s\rho_o(gh)^{0.5}} = \frac{0.85}{\Psi} \tag{20}$$

This simple model predicts the burning rate within 19.7% for all cribs and within 17.7% for the cribs with $b = 0.16$ cm sticks. Note that this relation does not have the same exponential dependency as the best-fit curve by Thomas in Eq. 9 [37]. There are several possible reasons for this. As the definition of the parameter Ψ essentially considers only a single shaft, Thomas excluded cribs with a large ratio of horizontal to vertical dimensions (l/h) as these cribs were reasoned to violate the assumption that the burning behavior of cribs is governed by the flow through the vertical shafts [37]. It is unclear what threshold Thomas used for this ratio, but the data from all cribs tested here is included in Figure 5 and is clearly predicted well from the relation in Eq. 20. This indicates that as long as there is sufficient vertical gap below the crib, the burning rate of all cribs, regardless of aspect ratio, is indeed governed by the vertical flow through the shafts as first suggested by Block [31, 32]. This may not have been appreciated before because, as will be discussed below, the critical vertical gap for these large aspect ratio cribs had been seriously underestimated. The primary data source for the correlation of Thomas was the experiments of O'Dogherty and Young [35], yet these authors did not specify the vertical gap separating the bottom of the crib from the solid floor below (d). Additional experimental factors may also contribute to the discrepancy. O'Dogherty and Young used a different species of wood with a much higher moisture content, and more importantly, used a different ignition technique. They ignited their cribs with a small pan of alcohol in the center of the crib (suggesting some unknown, but crucial, gap between the crib and the ground existed to insert the pan). Block had noted however that the burning rate was affected by the size of the ignition pan for pan sizes smaller than the base of the crib [31, 32].

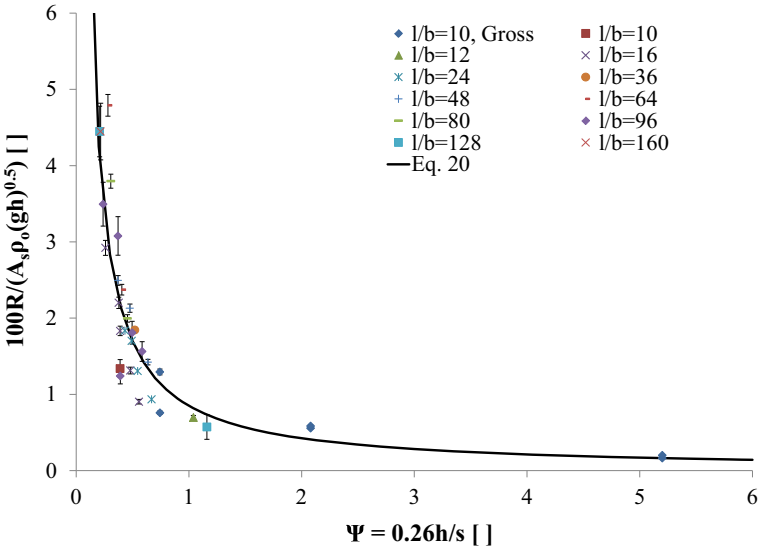

Figure 5. Measured maximum burning rate (R_{max}) compared to Thomas (Eq. 20).

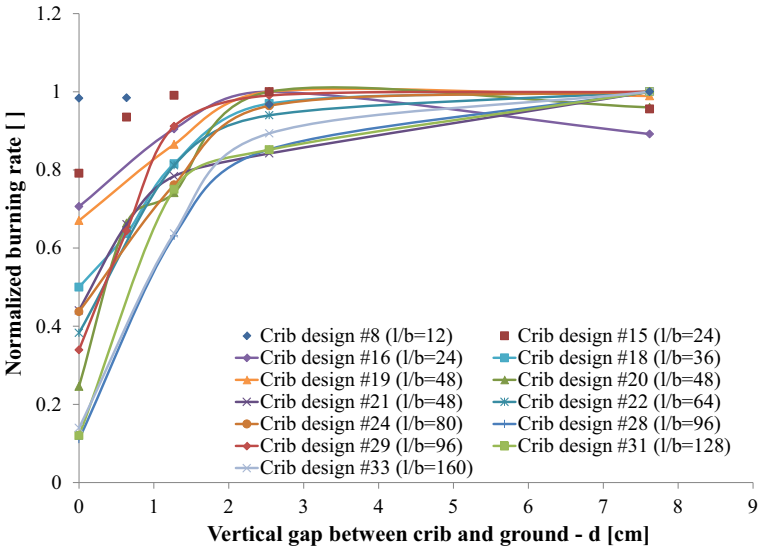

Figure 6. Normalized burning rate (R/R_{max}) as a function of the vertical gap between the crib and the ground (d).

4.4. *Effect of Vertical Gap Between Ground and Crib Base*

As mentioned above, the only study in the literature found to have examined the effect of the vertical gap (d) was that of Block [31, 32]. In his series of experiments with five crib designs with (l/b) of 10, Block determined that the critical vertical gap between the crib and the ground (d) was 1.27 cm (0.5'') with only a maximum change in the burning rate of 15%. As shown in Table 2 and Figure 6, in most cases a much larger critical vertical gap and subsequent change in the burning rate was seen with the wide variety of cribs tested here. The burning rate of cribs with l/b equal to 12 was virtually insensitive to the vertical gap. In fact, a slight decrease in the burning rate was seen for the largest gap tested (d = 7.62 cm), possibly due to increased convective or radiative heat losses. As the ratio of l/b increases, however, the effect of that vertical gap drastically increases. In fact, at l/b equal to or larger than 96, the difference was nearly 90%. This decrease in burning rate is seen visually as well. As shown in Figure 7, cribs with a l/b ratio equal to or greater than 48 burn as a propagating region from the outside edges inward when the vertical gap is small (0 cm to 1.27 cm). As the vertical gap increases, the cribs begin to burn simultaneously, in a similar fashion to the cribs with l/b less than 48. It is quite apparent that as the l/b ratio increases, a significant portion of

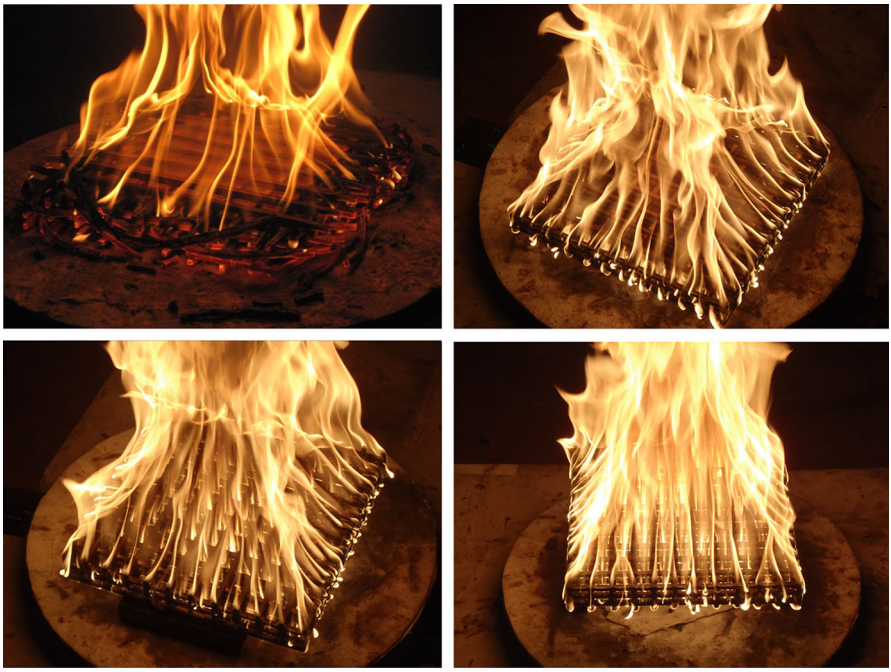

Figure 7. Crib design #20 at various vertical gaps between the ground and crib bottom (d). *Top left* 0 cm, *top right* 1.27 cm, *bottom left* 2.54 cm, *bottom right* 7.62 cm. With d = 0 cm and 1.27 cm, the crib burned from the outer edge toward the middle.

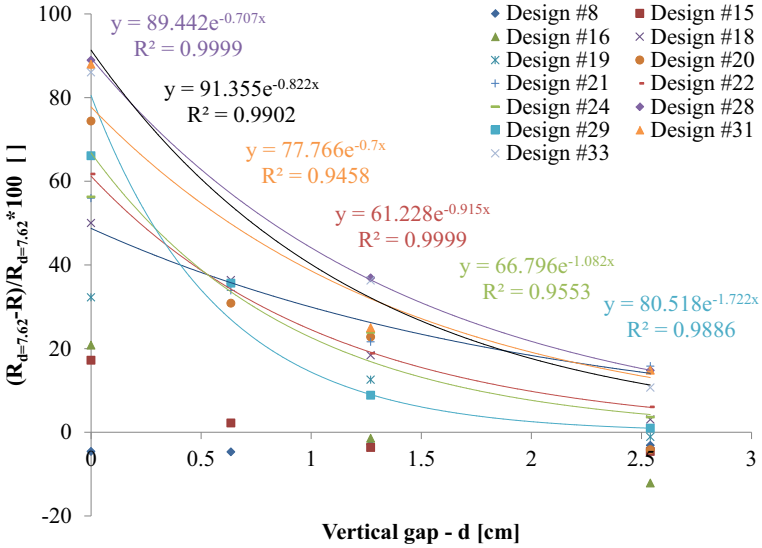

Figure 8. Percent change in the burning rate compared to the maximum vertical gap as the gap decreases.

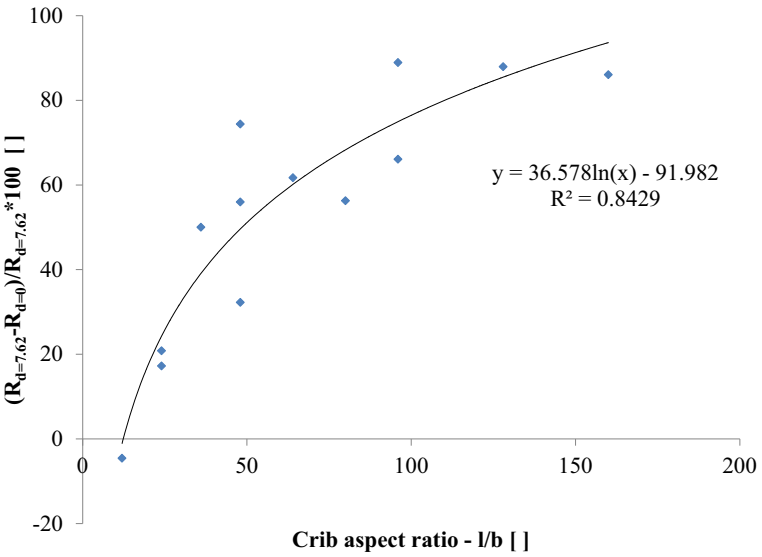

Figure 9. Maximum percent change in burning rate seen as the vertical gap changes as a function of aspect ratio.

the required oxidizer comes from the bottom of the crib, even for supposedly loosely-packed cribs. By looking at Figrue 6, it is apparent that the critical vertical gap (d) with large aspect ratios is more like 2.54 cm (1''), or in some cases, 7.62 cm (3'').

Because there is such as large change in the burning rate with vertical gap, it would be useful to have a correction factor to adjust the predicted burning rate for use in wildland fire models. In performing some exploratory data analysis, several trends stood out. As alluded to above, the change in the burning rate was related to both the aspect ratio and the vertical gap distance. Figure 8 shows the burning rate (R) at a given vertical gap (d) compared to the largest gap tested ($R_{d\ =\ 7.62\ \mathrm{cm}}$). Though the coefficient varies somewhat, the burning rate appears to decrease exponentially and be approximately proportional to e^{-d}. Figure 9 shows the maximum change seen in the burning rate (evaluated as $(R_{d\ =\ 7.62\ \mathrm{cm}} - R_{d\ =\ 0\ \mathrm{cm}})/R_{d\ =\ 7.62\ \mathrm{cm}}$) as a function of the aspect ratio of the crib. Here, also, a clear logarithmic trend is seen.

As a correlation of the form proposed by Thomas [37] was demonstrated to be the most appropriate for wildland fuels, a correction factor to this relation (Eq. 20) is developed that combines the effect of both the aspect ratio of the crib (l/b) and the vertical gap between the crib and the ground (d). The functional form of the effect of the vertical gap was assumed to be the same as above, e^{-d}, while the correlation in Figure 9 was redone to include the predicted value rather than the measured maximum value, $(R_{Predicted} - R_{d\ =\ 0})/R_{Predicted}$. Figure 10 shows the percent change from the calculated value of Eq. 20 as both the aspect ratio and vertical gap changes. The intercept was forced through zero as there should be no correction to the predicted value at sufficiently large vertical gaps.

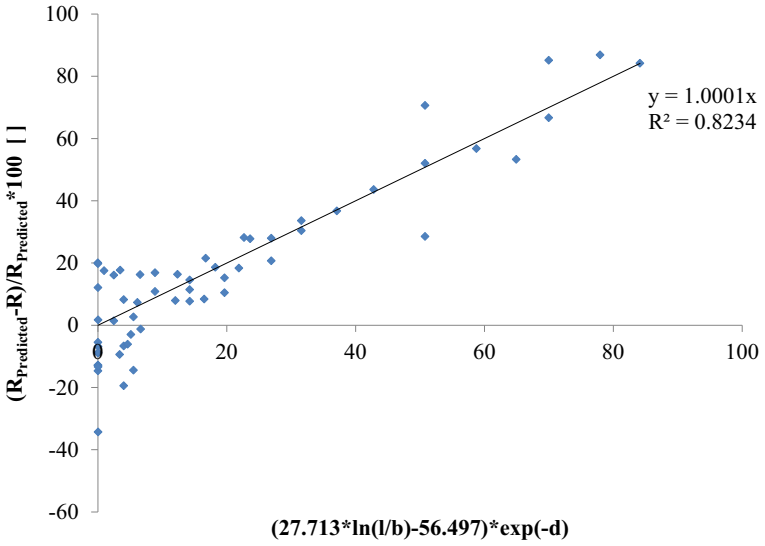

Figure 10. Change in the predicted value due to vertical gap (d) and aspect ratio (l/b) effects.

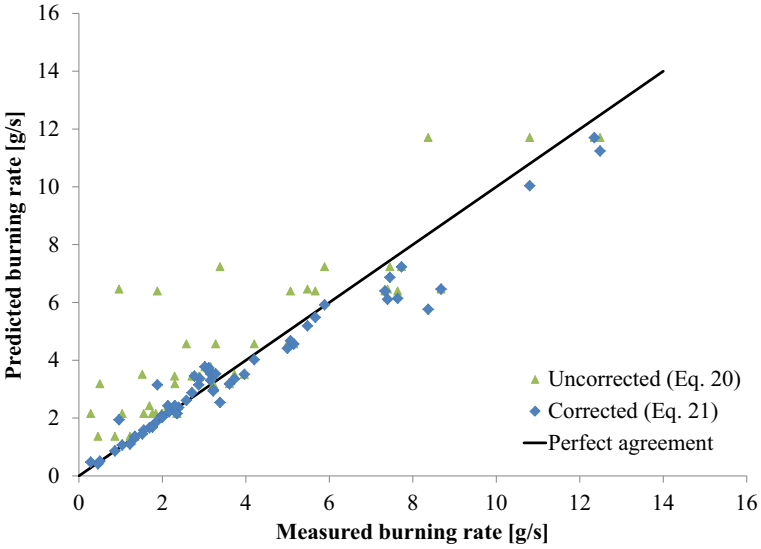

Figure 11. Measured burning rates compared to predicted values both with and without the correction in Eq. 21.

At an x-axis value of zero, the scatter in the data is due to the mismatch between the predicted and measured values. As the value of the x-axis increases, the spread of the data remains within the same range (±20%). The calculated burning rate taking into account the vertical gap is thus

$$R = R_{Predicted}\left\{1 - \left[0.277 \ln\left(\frac{l}{b}\right) - 0.565\right] \exp(-d)\right\} \tag{21}$$

where $R_{Predicted}$ is from Eq. 20. As one would expect, Figure 11 shows that this relation (Eq. 21) corrects the prediction so that it matches the measured data quite well, particularly compared to the uncorrected prediction (Eq. 20).

5. Conclusions and Future Work

The crib-burning literature was evaluated for purposes of predicting the burning rate of wildland fuel beds. Experiments were conducted to supplement the limited crib data from the literature by varying stick dimension, arrangement, aspect ratio, and vertical gap distance between the crib base and ground. Three correlations were considered for their applicability to cribs that would more closely resemble wildland fuel beds. Wildland fuels are characterized by thin fuel elements (ex. pine needle diameter $b \sim 1$ mm) which results in fuel beds with a large aspect ratio (l/b). It was found that a correlation in the form proposed by Thomas in [37] was the most suitable for such fuel beds. The critical vertical gap was shown to be much larger than previously thought, with a much larger effect on the burn-

ing rate. A correction factor was developed to adjust the predicted burning rate for vertical gaps that are less than the critical value. The strong influence of critical height on burning rates offers some insight into a source of variation among crib experiments reported in the literature that did not specify this parameter [28, 29, 34, 35].

Before these findings can be applied to the field, three important steps must be taken. The first, the effect of a forced flow on the burning rate must be examined to evaluate wind effects common to wildland fires. Second, the effect of moisture content must also be evaluated. And finally, measurements of actual wildland fuels must be translated into relevant crib-related parameters. The correlation suggested by this study shows that burning rate requires some known or easily determined properties of the fuel bed, such as fuel bed height (h) and surface area (A_s), but also some more challenging properties, such as the spacing between fuel elements (s). For ground fuels like the needle layer on the forest floor, this spacing is going to be relatively homogenous. However, shrubs and trees often have needles and leaves in clumps on branches, so there is no single value for spacing between the fuel elements. Experiments with real wildland fuels will help determine whether an average or effective fuel spacing will be an appropriate assumption.

Once the burning rate of wildland fuels is better understood, other aspects of wildland fire behavior will become more clear. For example, if the fuel loading and the burning rate of the fuel structure are known, the fireline intensity and flame zone depth can be estimated. The fireline intensity is related to the flame length [38, 39], which has been shown to characterize the fluid dynamics and convective heat transfer that spreads the fire [40]. Thus the fire spread rate can be better predicted with a better understanding of the burning rate.

One important complexity of wildland fires that is often overlooked is that most wildland fuels are not homogeneously distributed or continuous. Wildland fuels often occur in clumps, such as clumps of native grasses, shrubs, or trees. The residence time of the fire at a particular fuel clump can be determined from the burning rate of that fuel structure. This residence time is itself an important consideration for fire spread—if the residence time for a fuel structure is less than the ignition time for the next structure, the fire won't spread. This is of particular concern when discussing the thresholds for spread of canopy fires in conifer forests and shrublands, a currently poorly understood aspect of wildland fire. And finally, this residence time is also important for fire ecologists when evaluating fire effects. An important key to predicting tree mortality is the duration of heating.

Acknowledgments

The authors wish to thank James McGuire, Jennifer Kennedy, and Sophia Vernholm for their tireless and careful construction of the cribs and Cyle Wold for setting up the data acquisition system. Funding for this work was provided by the National Fire Decision Support Center.

References

1. Scheffey JL, Williams FW (1991) The extinguishment of fires using low flow water hose streams—part I. Fire Technol J 27(2):128–144. doi:10.1007/BF01470864
2. Forssell EW, Back GG, Beyler CL, DiNenno PJ, Hansen R, Beene D (2001) An evaluation of the international maritime organization's gaseous agents test protocol. Fire Technol J 37(1):37–67. doi:10.1023/A:1011697419034
3. Bill RG, Kung H-C, Anderson SK, Ferron R (2002) A new test to evaluate the fire performance of residential sprinklers. Fire Technol J 38(2):101–124. doi:10.1023/A:1014407200101
4. Beyler C, Dinaburg J, Mealy C (2014) Development of test methods for assessing the fire hazards of landscaping mulch. Fire Technol J 50(1):39–60. doi:10.1007/s10694-012-0264-y
5. Cruz MG, Gould JS, Alexander ME, Sullivan AL, McCaw WL, Matthews S (2015) A guide to the rate of fire spread models for Australian vegetation. Australasian Fire and Emergency Service Authorities Council Ltd. And Commonwealth Scientific and Industrial Research Organisation., Melbourne, Vic. (http://www.csiro.au/en/Research/LWF/Areas/Landscape-management/Bushfire/Fire-spread-models)
6. Canada. Forestry Canada. Fire Danger Group, Canada. Forestry Canada. Science, and Sustainable Development Directorate. "Development and Structure of the Canadian Forest Fire Behavior Prediction System". Vol. 3. Forestry Canada, Science and Sustainable Development Directorate, 1992
7. Andrews PL (1986) "BEHAVE: fire behavior prediction and fuel modeling system—burn subsystem, part 1," General Technical Report INT-194, Intermountain Research Station, USDA Forest Service
8. Heinsch FA, Andrews PL (2010) BehavePlus fire modeling system, version 5.0: design and features, General Technical Report RMRS-GTR-249, Rocky Mountain Research Station, USDA Forest Service
9. Finney MA (1998) "FARSITE: Fire area simulator—model development and evaluation," Research Paper RMRS-RP-4, Rocky Mountain Research Station, USDA Forest Service
10. Rothermel RC (1972) A mathematical model for predicting fire spread in wildland fuels," Research Paper INT-115, Intermountain Research Station, USDA Forest Service
11. Nelson RM Jr (2003) Reaction times and burning rates for wind tunnel headfires. Int J Wildland Fire 12:195–211
12. Anderson HE (1969) Heat transfer and fire spread, Research Paper INT-69, Intermountain Research Station, USDA Forest Service
13. Albini FA (1976) Estimating wildfire behavior and effects, General Technical Report INT-30, Intermountain Research Station, USDA Forest Service
14. Reinhardt ED, Keane RE, Brown JK (1997) First Order Fire Effects Model: FOFEM 4.0, user's guide, General Technical Report INT-GTR-344, Intermountain Research Station, USDA Forest Service
15. Albini FA, Reinhardt ED (1995) Modeling ignition and burning rate of large woody natural fuels. Int J Wildland Fire 5(2):81–91
16. Albini FA, Brown JK, Reinhardt ED, Ottmar RD (1995) Calibration of a large fuel burnout model. Int J Wildland Fire 5(3):173–192
17. Albini FA (1980) Thermochemical properties of flame gases from fine wildland fuels, Research Paper INT-243, Intermountain Research Station, USDA Forest Service

18. Burrows ND (2001) Flame residence time and rates of weight loss of eucalypt forest fuel particles. Int J Wildland Fire 10:137–143
19. Fons WL, Clements HB, George PM (1963) Scale effects on propagation rate of laboratory crib fires. Symposium (International) on Combustion vol. 9, no. 1, pp. 860–866
20. Steward FR, Tennankore KN (1981) The measurement of the burning rate of an individual dowel in a uniform fuel matrix. Symposium (International) on Combustion vol. 18, no. 1, pp. 641–646
21. Albini FA (1967) A physical model for firespread in brush. Symposium (International) on Combustion vol. 11, no. 1, pp. 553–560
22. Weise DR, White RH, Beall FC, Etlinger M (2005) Use of the cone calorimeter to detect seasonal differences in selected combustion characteristics of ornamental vegetation. Int J Wildland Fire 14:321–338
23. Dibble AC, White RH, Lebow PK (2007) Combustion characteristics of north-eastern USA vegetation tested in the cone calorimeter: invasive versus non-invasive plants. Int J Wildland Fire 16:426–443
24. Schemel CF, Simeoni A, Biteau H, Rivera JD, Torero JL (2008) A calorimetric study of wildland fuels. Exp Thermal Fluid Sci 32:1381–1389
25. Simeoni A, Bartoli P, Torero JL, Santoni PA (2011) On the role of bulk properties and fuel species on the burning dynamics of pine forest litters. In: Fire safety science—proceedings of the tenth international symposium, pp. 1401–1414
26. Bartoli P, Simeoni A, Biteau H, Torero JL, Santoni PA (2011) Determination of the main parameters influencing forest fuel combustion dynamics. Fire Saf J 46:27–33
27. Simeoni A, Thomas JC, Bartoli P, Borowieck P, Reszka P, Colella F, Santoni PA, Torero JL (2012) Flammability studies for wildland and wildland-urban interface fires applied to pine needles and solid polymers. Fire Saf J 54:203–217
28. Byram GM, Clements HB, Elliott ER, George PM (1964) An experimental study of model fires, Technical Report No. 3, Forest Service, USDA Southeastern Forest Experiment Station
29. Anderson HE (1990) Relationship of fuel size and spacing to combustion characteristics of laboratory fuel cribs,'' Research Paper INT-424, Intermountain Research Station, USDA Forest Service, July 1990
30. Gross D (1962) Experiments on the burning of cross piles of wood. J Res Natl Bur Stand C 66c(2):99–105
31. Block JA (1970) A theoretical and experimental study of nonpropagating free-burning fires. Ph.D. Thesis, Harvard University, Cambridge, MA
32. Block JA (1971) A theoretical and experimental study of nonpropagating free-burning fires. Symposium (International) on Combustion vol. 13, pp. 971–978
33. Heskestad G (1973) Modeling of enclosure fires. Symposium (International) on Combustion vol. 14, pp. 1021–1030
34. Delichatsios MA (1976) Fire growth rates in wood cribs. Combust Flame 27:267–278
35. O'Dogherty MJ, Young RA (1964) Miscellaneous experiments on the burning of wooden cribs,'' Fire Research Note No. 548, Fire Research Station, Boreham Wood, Herts
36. Smith PG, Thomas PH (1970) The rate of burning of wood cribs. Fire Technol 6(1):29–38. doi:10.1007/BF02588857
37. Thomas PH (1973) Behavior of fires in enclosures—some recent progress. Symposium (International) on Combustion vol. 14, pp. 1007–1020
38. Byram GM (1959) Combustion of forest fuels. In: Davis KP (ed) Forest fire: control and use McGraw-Hill Book Co, New York

39. Rothermel RC, Deeming JE (1980) Measuring and interpreting fire behavior for correlation with fire effects, General Technical Report INT-93, Intermountain Research Station, USDA Forest Service, November 1980
40. Finney MA, Cohen JD, Forthofer JM, McAllister SS, Gollner MJ, Gorham DJ, Saito K, Akafuah NK, Adam BA, English JD (2015) Role of buoyant flame dynamics in wildfire spread. Proc Natl Acad Sci . doi:10.1073/pnas.1504498112